frontiers | Frontiers in Energy Research

TYPE Original Research
PUBLISHED 17 September 2024
DOI 10.3389/fenrg.2024.1421212

OPEN ACCESS

EDITED BY
Joshuva Arockia Dhanraj,
Dayananda Sagar University, India

REVIEWED BY
Ioan Viorel Banu,
University of Bacău, Romania
Mohamed Salem,
University of Science Malaysia (USM), Malaysia
Mohammad Samiullah,
King Fahd University of Petroleum and Minerals, Saudi Arabia

*CORRESPONDENCE
Umit Cali,
umit.cali@ntnu.no
Taha Selim Ustun,
selim.ustun@aist.go.jp

RECEIVED 22 April 2024
ACCEPTED 28 August 2024
PUBLISHED 17 September 2024

CITATION
Lalhmachhuana R, Deb S, Datta S, Singh KR, Cali U and Ustun TS (2024) Multi-objective-based economic and emission dispatch with integration of wind energy sources using different optimization algorithms.
Front. Energy Res. 12:1421212.
doi: 10.3389/fenrg.2024.1421212

Multi-objective-based economic and emission dispatch with integration of wind energy sources using different optimization algorithms

R. Lalhmachhuana[1], Subhasish Deb[1], Subir Datta[1], Ksh. Robert Singh[1], Umit Cali[2,3]* and Taha Selim Ustun[4]*

[1]Department of Electrical Engineering, Mizoram University, Aizawl, Mizoram, India, [2]Department of Electric Energy, Norwegian University of Science and Technology, Trondheim, Norway, [3]School of Physics, Engineering and Technology, University of York, York, United Kingdom, [4]Fukushima Renewable Energy Institute, AIST (FREA), Koriyama, Japan

In this work, a study of economic and emission dispatch issues based on the multi-objective optimization is solved, and generation costs and emissions are reduced by utilizing multi-objective optimization techniques. This optimization is carried out in an IEEE-30 bus system, with and without the integration of wind energy sources, with equality and inequality constraints. The equality constraints are the power balance constraints, stipulating that to have an optimal solution, the generated power must be adequate to satisfy the load demand plus losses. The inequality constraints are a collection of limitations for active power generation, reactive power generation, generator bus voltage, and load bus voltage. To track the hourly load demand, a daily load profile is established using the IEEE-30 bus system. The generation costs and emissions in the system are optimized using multi-objective particle swarm optimization and multi-objective Ant–Lion Optimization approaches. In order to determine the goals' minimum values, a fuzzy min–max technique is applied. The values that have been minimized are then compared to determine how well wind energy integration has reduced the generation costs and emissions. Two case studies are performed in this work. For Case 1, the total generation costs and emissions using MOPSO are less, with a difference of $42.763, while MOALO has lower emissions, with a difference of 157.337 tons. For Case 2, with the implementation of wind energy, MOPSO has lower total generation costs, with a difference of $51.678, and lower emissions, with a difference of 459.446 tons.

KEYWORDS

multi-objective optimization, generation costs and emissions, wind power, economic dispatch, emission dispatch

1 Introduction

The urgent need to transform our energy generation portfolio arises from the combined pressures of environmental degradation, resource depletion, and climate change (Abdolrasol et al., 2021). Fossil fuels, while historically dominant, contribute significantly to greenhouse gas emissions, air pollution, and global warming, which have detrimental effects on ecosystems and human health. Transitioning to a greater share of renewable energy sources, such as wind, solar, and hydropower, is crucial to mitigate these impacts (Ulutas et al., 2020; Srinivasan et al., 2023).

TABLE 1 Load profile for 24 h.

Time of the day (Hr)	Real power demand (MW)	Time of the day (Hr)	Real power demand (MW)
01:00	79.3520	13:00	150.2020
02:00	62.3480	14:00	153.0360
03:00	59.5140	15:00	172.8740
04:00	59.5140	16:00	206.8820
05:00	62.0160	17:00	212.5500
06:00	93.5220	18:00	240.8900
07:00	167.2060	19:00	283.4000
08:00	172.8740	20:00	184.2100
09:00	133.1980	21:00	144.5340
10:00	127.5300	22:00	121.8620
11:00	130.3640	23:00	110.5620
12:00	136.0320	24:00	87.8540

Renewable energy offers a cleaner, more sustainable alternative, significantly reducing carbon footprints and helping stabilize global temperatures. Moreover, the decreasing costs and technological advancements in renewable energy make it an increasingly viable option for meeting the growing energy demands (Basu et al., 2022).

Introducing more renewable energy sources into the power grid presents several challenges that need to be addressed to ensure a reliable and efficient energy system (Ustun et al., 2011). One major challenge is the intermittent nature of renewable energy such as wind and solar power, which can lead to fluctuations in energy supply and require the development of advanced energy storage solutions or backup systems to maintain a steady power flow (Yarar et al., 2023). Additionally, the integration of distributed generation from renewables often necessitates upgrades to the existing grid infrastructure to handle variable inputs and ensure seamless connectivity. The variability in renewable energy sources can also complicate grid management and forecasting, requiring sophisticated algorithms and real-time monitoring to effectively balance supply and demand. Furthermore, the geographic dispersion of renewable energy installations can lead to transmission bottlenecks and increased costs for infrastructure development. Lastly, the incorporation of more renewables can impact power quality, as fluctuating inputs from sources like wind turbines and solar panels may introduce voltage and frequency instability, requiring additional measures to maintain consistent power quality and reliability across the grid (Latif et al., 2021). Addressing these challenges is crucial to fully realizing the benefits of renewable energy and ensuring a stable and efficient power system.

To enhance power quality, optimal power flow (OPF) is employed to achieve the best possible power flow. The economic and reliable operation of electrical systems is critically important. The OPF challenge typically aims to minimize objectives by adjusting the variables within the power system (Chen et al., 2019; Hoang Bao Huy et al., 2022). OPF often involves large-scale, nonconvex, nonlinear, mixed-integer, and highly constrained optimization problems (Ghasemi et al., 2014; Niu et al., 2014). Traditionally, the primary goal of OPF systems has been to reduce fuel costs. To maintain high electricity quality, utilities must also minimize transmission losses for economic reasons. Given the growing environmental concerns, emission levels should now be considered part of the objective function rather than merely a constraint (Zhang et al., 2016). With the increasing public awareness of environmental issues, the economic dispatch problem has evolved. The absolute minimum cost is no longer the sole objective. When power is generated from fossil fuels, it releases pollutants such as sulfur oxides and nitrogen oxides into the atmosphere. These pollutants not only harm the environment but also have adverse effects on human health, as well as on plants and animals (Surender Reddy, 2018).

A crucial tool for managing the distribution system is the power flow method, which is commonly referred to as the load flow method. Depending on the regulating capacities of transformers, condensers, alternators, and other equipment, load flow solutions offer insights into reactive power and real power losses, as well as voltage magnitudes and voltage angles at various nodes within the distribution system. Most load flow analyses in engineering focus on reducing production costs and operating the system efficiently (Chatuanramtharnghaka and Deb, 2020). This study simplifies the Newton–Raphson power flow solution approach, which is based on the principle of current balancing and involves a set of nonlinear equations. Despite the availability of several effective Newton–Raphson (NR)-based power flow solvers, challenges arise because the derivatives of the Jacobian matrix must be calculated. This study illustrates how the updating formulas for Jacobian matrices differ from those used in the traditional Newton–Raphson approach (Kulworawanichpong, 2010). Over the past few decades, renewable energy resources have addressed the growing demand in the energy market (Khan, 2009). Wind energy, in particular, has recently gained popularity due to its ability to generate electrical power (Manwell et al., 2010; Johnson, 1985). This growing interest is driven by efforts to reduce pollution and mitigate its harmful effects on the environment, given that fossil fuel-powered power plants are significant sources of greenhouse gas emissions.

Wind energy is an environmentally friendly renewable resource. The global interest in wind energy conversion systems, which generate electric power, has been rapidly increasing, with the average annual growth rate exceeding 25% over the past decade. To ensure that the wind energy conversion technology operates as efficiently as possible, it is crucial that wind turbines are precisely designed for their installation sites (Salih et al., 2012; Khalfallah and Koliub, 2007; Bencherif et al., 2014). Wind characteristics, such as direction and velocity, are influenced by various factors, including location and climate (Bianchi et al., 2007; Kala and Sandhu, 2016; Hamoudi et al., 2023). The ability of a wind turbine to generate electricity depends on several site-specific factors and the aerodynamic performance of its blades. Key factors include the average annual wind speed, blade pre-twist, pitch, attachment angle, and rotor swept area. Additionally, air density affects wind turbine performance and can vary with altitude and temperature (Wiratama et al., 2016; Kanchikere, 2012; Badran and Abdulhadi, 2009). When constructing a wind turbine, it is essential to consider several climatic factors, such as wind speed, turbine swept area, air density, site temperature, and tower height. The choice of the wind turbine should reflect the specific climatic characteristics of the site (Marimuthu and Kirubakaran, 2014; Nemes and Munteanu, 2012).

Nature-inspired optimization algorithms are particularly useful for renewable energy deployments in future power systems due to their

TABLE 2 Optimization of the IEEE-30 bus system using MOPSO.

Time	G1	G2	G3	G4	G5	G6	Power demand	Loss	Power generation	Generation cost	Emission
(Hr)	(MW)	(MW)	(MW)	(MW)	(MW)	(MW)	(MW)	(MW)	(MW)	($/hr)	(ton/hr)
01:00	60.7661	0	0	0	19.6616	0	79.352	1.0849	80.4277	204.029	253.263
02:00	51.477	0	0	0	11.6291	0	62.348	0.8281	63.1061	151.159	174.994
03:00	50.0677	0	0	0	10.3035	0	59.514	0.8572	60.3712	143.1	164.519
04:00	50.083	0	0	0	10.1872	0	59.514	0.7652	60.2702	142.517	164.514
05:00	53.7254	0	0	0	15.1404	0	68.016	0.8589	68.8657	169.427	194.352
06:00	74.1448	0	0	0	20.8125	0	93.522	1.43531	94.9573	242.172	371.737
07:00	63.3868	38.1323	20.9609	20.0652	11.7639	14.9381	167.2	2.0412	169.2472	440.153	388.849
08:00	65.4223	41.4407	22.7572	21.4639	11.9549	12	172.874	2.1682	175.0391	457.233	424.56
09:00	111.429	0	0	24.6286	0	0	133.198	2.8597	136.0577	354.522	826.467
10:00	106.346	0	0	23.8188	0	0	127.53	2.6346	130.1646	337.245	753.146
11:00	108.315	0	0	24.7445	0	0	130.364	2.6987	133.0596	346.152	782.487
12:00	117.693	0	0	21.4938	0	0	136.032	3.1611	139.1873	361.039	912.799
13:00	58.0696	36.9459	17.5253	15.4773	11.8328	12	150.202	1.6489	151.8509	384.947	325.917
14:00	57.1829	34.3743	20.1429	19.6642	10	13.4	153.036	1.7343	154.7643	397.285	320.027
15:00	63.3829	43.7497	20.5174	22.2421	12.0686	12.9724	172.874	2.0591	174.9331	458.101	416.133
16:00	81.759	47.3969	23.7238	25.478	15.9231	15.6697	206.882	3.0686	209.9506	565.216	628.045
17:00	79.8906	44.5685	21.1404	33.7688	18.2942	18.1236	212.55	3.2513	215.7861	590.635	616.646
18:00	87.3038	46.1804	26.6111	33.75	23.9829	26.8192	240.89	3.7608	244.6476	696.153	741.56
19:00	119.826	53.936	26.1921	35	25.659	29.0443	283.4	6.2576	289.6576	833.487	1,230.86
20:00	72.1583	40.9228	18.2367	24.507	15.6146	15.3935	184.21	2.6259	186.8329	493.487	486.386
21:00	61.7913	34.5432	16.75	11.25	10	12	144.534	1.8004	146.3344	363.236	337.089
22:00	103.028	0	0	21.309	0	0	121.862	2.47751	124.3365	318.901	703.174
23:00	93.9665	0	0	0	18.6519	0	110.526	2.0924	112.6184	225.396	328.217
24:00	69.7236	0	0	0	19.4276	0	87.854	1.308	89.15124	285.698	583.099

ability to efficiently handle complex, nonlinear, and multidimensional problems in optimizing energy systems. Their ability to balance exploration and exploitation makes them well-suited for optimizing various aspects of renewable energy systems, such as resource allocation, grid integration, and system design, ultimately leading to more robust and efficient power system configurations. Some examples of effective applications for power system issues are the salp swarm algorithm (Latif et al., 2020), butterfly optimization (Dey et al., 2020), biogeography-based algorithm (Chauhan et al., 2021), sine cosine algorithm (Nayak et al., 2023), chaotic selfish-herd optimization (Barik et al., 2021), flower pollination algorithm (Hussain et al., 2020), satin bowerbird algorithm (Farooq et al., 2022), moth flame optimization algorithm (Singh et al., 2021), COVID-19-based optimization (Safiullah et al., 2022), and slime mold algorithm (Das et al., 2022). Similarly, multi-objective ant lion optimizer (MOALO) is inspired by the hunting behavior of ant lions, particularly their interactions with prey such as ants in nature. MOALO represents an extension of the ant lion optimizer (ALO) and operates similarly to other population-based optimization techniques, such as multi-objective particle swarm optimization (MOPSO) and multi-objective genetic algorithm optimization (MOGOA) (Mirjalili et al., 2016). The particle swarm optimization (PSO) algorithm, in contrast, is modeled after the fluttering motion of flocks of birds. Observations of bird flocks reveal that they follow specific patterns while searching for food, allowing them to stay close to available resources. In PSO, the individual's local best and the global best influence the position and velocity of the search process. This algorithm involves creating a population of particles and evaluating each particle's performance individually within the search space (Coello Coello et al., 2004).

The novel aspects and contribution of the work are summarized below:

- The multi-objective optimization algorithm-based fuzzy min–max approach with competing objectives is utilized to address the multi-objective optimal power flow problem. The meta-heuristic algorithm is utilized to capture the numerous optimal solutions in its final population when the issue is

TABLE 3 Optimization of the IEEE-30 bus system using MOALO.

Time	G1	G2	G3	G4	G5	G6	Power demand	Loss	Power generation	Generation cost	Emission
(Hr)	(MW)	(MW)	(MW)	(MW)	(MW)	(MW)	(MW)	(MW)	(MW)	($/hr)	(ton/hr)
01:00	60.0747	0	0	0	20.3403	0	79.352	1.073	80.415	205.047	249.089
02:00	51.25	0	0	0	11.8566	0	62.348	0.7586	63.1066	151.434	173.726
03:00	50.1163	0	0	0	10.1265	0	59.514	0.738	60.2428	142.595	164.675
04:00	50.154	0	0	0	10.1262	0	59.514	0.7662	60.2802	142.683	164.918
05:00	52.193	0	0	0	16.6442	0	68.016	0.881	68.8372	171.46	186.019
06:00	74.3374	0	0	0	20.7373	0	93.522	1.5557	95.0747	242.36	373.443
07:00	63.9242	32.9605	21.1404	20.0638	12.5615	18.6738	167.206	2.1181	169.3241	443.87	378.18
08:00	64.1051	37.365	22.212	22.6141	13.352	15.1963	172.874	2.0644	174.8446	460.12	401.107
09:00	112.951	0	0	23.1641	0	0	133.198	2.9274	136.1155	353.504	845.416
10:00	111.154	0	0	19.2107	0	0	127.53	2.8354	130.3645	334.152	811.889
11:00	108.89	0	0	24.1925	0	0	130.964	2.721	133.082	345.749	789.341
12:00	113.541	0	0	25.4686	0	0	136.032	2.9774	139.0094	363.607	859.068
13:00	62.4564	33.1695	18.4415	10.335	15.3303	12.3239	150.202	1.8547	152.0567	383.653	345.542
14:00	62.3749	35.3518	20.3177	11.6097	12.4256	12.7381	153.036	1.7849	154.8179	391.458	354.832
15:00	79.7161	33.0844	18.5435	16.598	13.5011	14.1944	172.874	2.7736	175.6376	449.272	510.416
16:00	70.7307	43.14	27.3133	32.8029	15.675	19.9152	206.882	2.701	209.5771	580.637	531.093
17:00	73.8397	50.7458	27.1699	29.1736	17.3285	17.5273	212.55	3.2408	215.7848	596.97	588.847
18:00	86.1193	52.9118	30.1329	24.6002	23.7506	26.9483	240.89	3.5761	244.463	697.874	751.307
19:00	105.413	66.3551	31.2651	30.2133	25.3641	29.8825	283.4	5.0961	288.493	847.982	1,106.07
20:00	72.94	41.2584	16.7728	15.7412	18.3121	21.5922	184.21	2.4067	186.6167	495.156	488.536
21:00	58.5522	27.5747	17.3165	11.915	15.9886	14.8498	144.534	1.6658	146.1968	371.908	298.94
22:00	101.804	0	0	22.5041	0	0	121.862	2.446	124.308	319.835	689.316
23:00	94.7175	0	0	17.994	0	0	110.526	2.1885	112.7115	285.154	591.181
24:00	68.3555	0	0	0	20.8307	0	87.854	1.3322	89.1862	227.573	318.552

TABLE 4 Wind turbine Swt-3.2-113 data sheet (El-Ahmar et al., 2017).

Type	3-bladed, horizontal axis	Nominal power	3,200 kW
Diameter	113 m	Frequency	50 Hz or 60 Hz
Swept area	10,000 m^2	Hub height	83.5–115 m
Speed range	4–16.5 rpm	Cut-in wind speed	3–5 m/s
Blade length	55 m	Rated wind speed	9–10 m/s
Voltage	690 V	Cut-out wind speed	32 m/s

formulated for the simultaneous optimization of several competing objectives.

- The MOPSO algorithm was found to be extremely effective and competitive in locating a precise estimate of the Pareto optimal front with high distribution across all objectives. Additionally, strong convergence and extensive exploration characteristics of MOPSO produce, respectively, accurate estimated solutions and a good distribution. The procedure for choosing targets and maintaining archives also promotes research and the sharing of solutions.

TABLE 5 Wind speed for the 24-h period.

Time of the day (Hr)	Wind speed (m/s)	Time of the day (Hr)	Wind speed (m/s)
01:00	5.7	13:00	6.9
02:00	4.5	14:00	7.9
03:00	4.5	15:00	8.5
04:00	5.6	16:00	8.4
05:00	3.9	17:00	10.5
06:00	5.6	18:00	13.6
07:00	4.6	19:00	10.4
08:00	3.2	20:00	8.9
09:00	5.3	21:00	7.5
10:00	7.8	22:00	6.8
11:00	7.7	23:00	3.8
12:00	7.0	24:00	4.8

2 Multi-objective-based problem formulation

We take into account two objectives in this multi-objective problem that are detailed below:

2.1 Fuel cost

The formulation of the power generation fuel cost is shown in Equation 1

$$F_1 = \sum_{i=1}^{NG} \left(a_i + b_i P_{G,i} + c_i P_{G,i}^2 \right), \tag{1}$$

where the number of generators is denoted by NG (which is 6). $P_{G,i}$ refers to the ith generator's active power output. a_i, b_i, and c_i denote the ith generator's cost coefficients.

2.2 Emission

When thermal units employing fossil fuels produce electricity, atmospheric pollutants are emitted. Equation 2 gives the total harmful gas emissions (ton/hr):

$$F_2 = \sum_{i=1}^{NG} \left[\left(a_i + \beta_i P_{G,i} + \gamma_i P_{G,i}^2 + \omega_i e^{\left(\mu_i P_{G,i}\right)} \right) \right], \tag{2}$$

where α_i, β_i, γ_i, and μ_i denote the ith generator's emission characteristics.

2.3 Objective function

The proposed objective function aims to reduce generation costs and emissions. It is multi-objective-based. Consequently, the objective function is expressed as shown in Equation 3

$$Fobj\,min = \left(\sum (F_1 + F_2) \right)_{min}. \tag{3}$$

2.4 Constraints

Constraints can be defined as a condition that a solution must satisfy in solving an optimization problem.

2.4.1 Equality constraint

It is described as the power balance constraint, which stipulates that to have an optimal solution, the generated power needs to be adequate to satisfy the load demand plus losses. The formula for the power balance equation is shown in Equation 4 (Chatuanramtharnghaka and Deb, 2020)

$$P_{Gen,t} = P_{D,t} + P_{Loss,t,} \tag{4}$$

where $P_{D,t}$, $P_{Gen,t}$, and $P_{Loss,t}$ are the power demand, thermal power generated, and power loss, respectively, at time t.

2.4.2 Power balance constraint for the wind energy source

Considering the integration of wind energy, in each dispatch time period, the power balance equation is represented as shown in Equation 5

$$P_{Gen,t} + P_{wind,t} = P_{D,t} + P_{Loss,t}, \tag{5}$$

where $P_{D,t}$, $P_{Gen,t}$, $P_{Loss,t}$, and $P_{wind,t}$ are the power demand, thermal power generated, power loss, and wind power generated, respectively, at time t.

2.5 Inequality constraint

2.5.1 Generator constraints

The following constraints set a restriction on how much voltage, active power, and reactive power can be generated for the system as shown in Equations 6, 7:

$$V_{Gp}^{\min} \le V_{Gp} \le V_{Gp}^{\max}; \quad p = 1, \ldots\ldots, N_G, \tag{6}$$

$$P_{Gp}^{\min} \le P_{Gp} \le P_{Gp}^{\max}; \quad p = 1, \ldots\ldots, N_G. \tag{7}$$

The voltage magnitude and real power production are denoted by V_{Gp} and P_{Gp}, respectively. N_G stands for the "generating unit number."

2.5.2 Security constraints

The limitations on the line power flow and the load bus voltage are known as security constraints as in Equations 8, 9:

$$V_{Lr}^{\min} \le V_{Lr} \le V_{Lr}^{\max}; \quad r = 1, \ldots\ldots, N_L, \tag{8}$$

$$S_{Lr} \le V_{Lr}^{\max}, \tag{9}$$

where S_{lr} is the power at branch N_{BR} and V_{Lr} is the load bus r voltage magnitude.

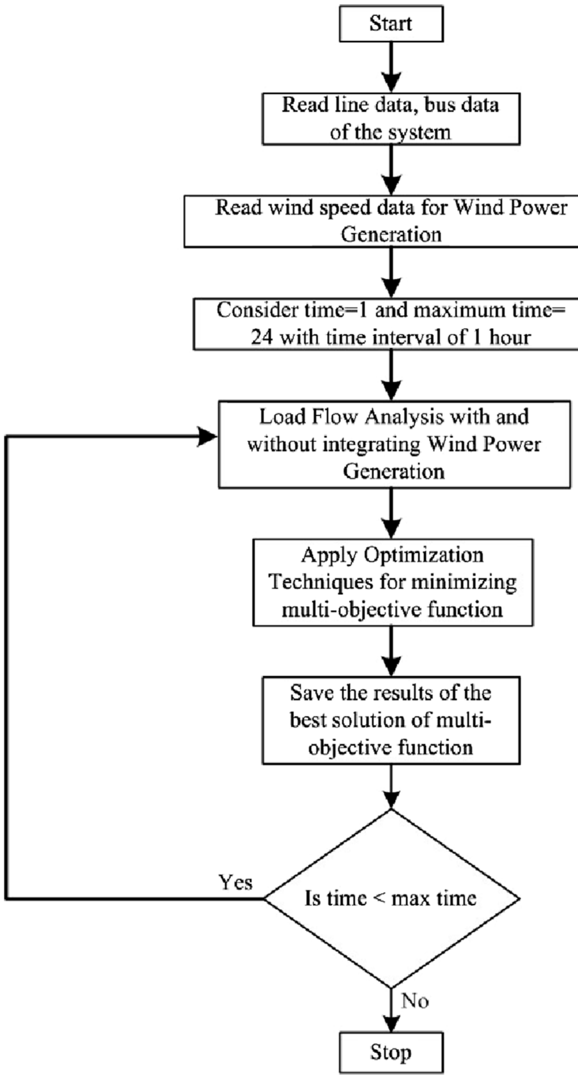

FIGURE 1
Flowchart of the proposed work.

2.6 Wind turbine modeling

The air's power output may be calculated using Equation 10 (El-Ahmar et al., 2017):

$$P_{wind} = \frac{1}{2}(\rho A v^2)v = \frac{1}{2}\rho A v^3. \quad (10)$$

The relationship between wind energy and speed is described as in Equation 11: (Burton et al., 2011):

$$P_{wind} = \begin{cases} 0 & v \le v_{cut-in} \text{ or } v \ge v_{cut-off} \\ \frac{1}{2}C_p \rho A v^3 & v_{cut-in} < v \le v_{rated} \\ P_{rated} & v_{rated} < v < v_{cut-off} \end{cases}, \quad (11)$$

where P_{wind}, v_{cut-in}, $v_{cut-off}$, v_{rated},and P_{rated} are the wind power generation, cut-in wind velocity, cut-off wind velocity, rated wind velocity, and rated power of the turbines, respectively.

3 Multi-objective optimization and work flowchart

3.1 Multi-Objective Ant Lion Optimization

The multi-objective ant lion optimizer (MOALO) was proposed by Seyedali Mirjalili, Pradeep Jangir, and Shahrzad Saremi in 2016. The optimization algorithm mimics the hunting methods of ant lion and how they interact with their prey, such as ants, in the nature. The MOALO is an extended edition of the ant lion optimizer (ALO). This optimization shares some similarity with the other population-based optimization techniques like the MOPSO and MOGOA (Mirjalili et al., 2016).

3.2 Multi-objective particle swarm optimization

The algorithm was modeled based on the fluttering motion of a flock of birds. A group of birds were observed to follow a pattern in their quest for food, and then they could remain next to the nearest resources. The individual's local and global best have an impact on the position and speed of the search process. This program uses the idea of creating a population and evaluating each particle's performance in the search space (Coello Coello et al., 2004).

The multi-objective particle swarm optimization algorithm is as follows:

1. Initialize a population of size *Np* (size of the population depends on the complexity of the problem).
2. Initialize particle velocity. Consideration of zero velocity at the beginning.
3. Evaluation of the number of particles in the population.
4. Save the evaluated result and particle position in the repository.
5. The location of particles in the search space is identified through a hypercube. Each particle is defined as per the values of the objective function accordingly.
6. Initialization of each particle memory.

For j = 0 to maximum.
Best Position(j) = Population(j).

7. Update velocity of the particles using the following equation:

$Vel(j) = w \times Vel(j) + R_1 \times [BestPosition(j) + Population(j)] + R_2 \times [REP(k)\text{-}Population(j)]$

Here, w is inertia weight [0.3–1]. R_1 and R_2 are random numbers [0–1], and $REP(k)$ is the repository value.

8. Performance of roulette wheel selection is done to select the hypercube. Following that within the hypercube, the random selection of the particle is done.
9. Updated velocity is considered to evaluate the new position.

Population(j) = Population(j) + Vel(j)

10. Particles in the population are evaluated for the objective function.
11. The repository is updated. The elimination of the non-dominated vectors is done considering the new vectors.
12. The particles positions are updated if the current position is better than the previous position.

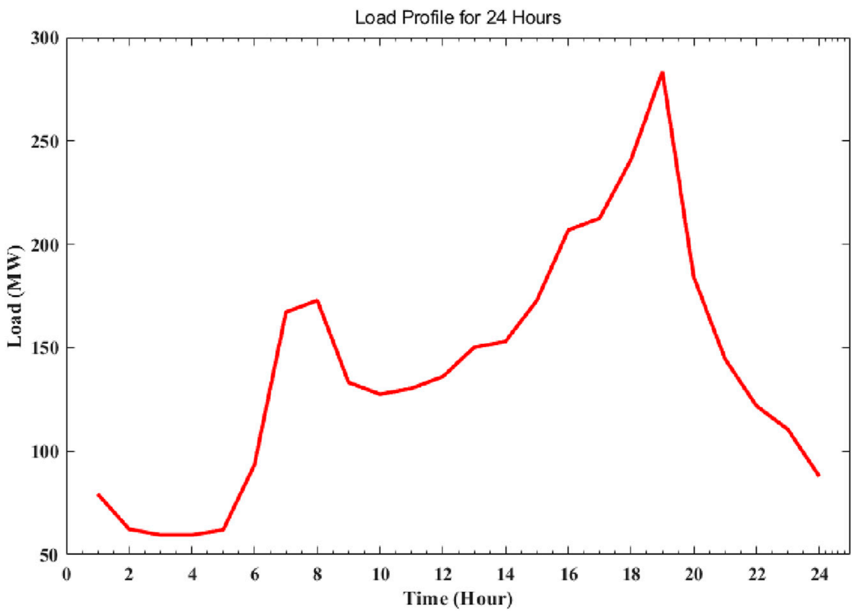

FIGURE 2
Daily load profile.

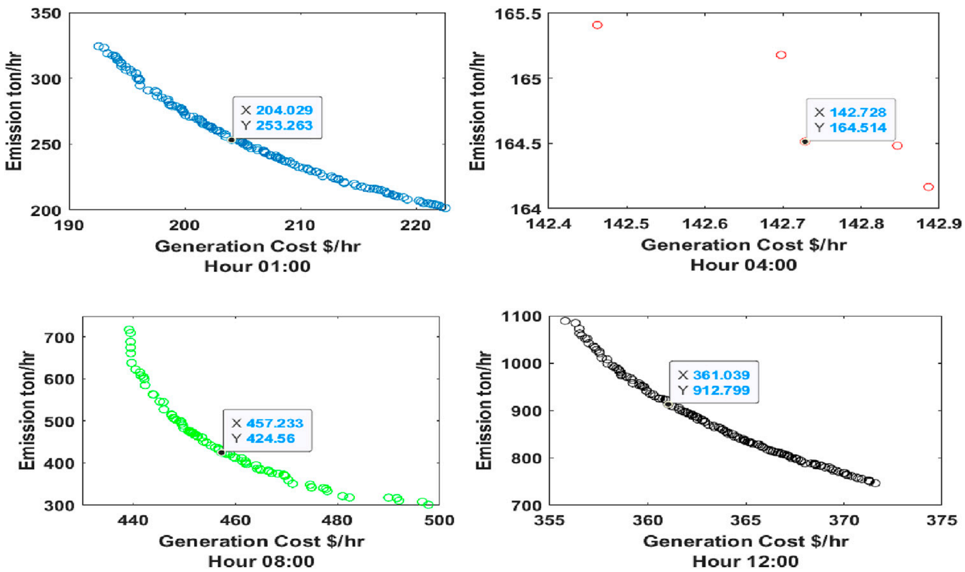

FIGURE 3
Pareto optimal curves for hours 01:00, 04:00, 08:00, and 12:00 in the IEEE-30 bus system (MOPSO).

Best Position(j) = Population(j)

13. Increase in the generation.
14. END the loop considering maximum generation.

3.3 Work flowchart of the proposed work

The work flowchart is shown in Figure 1. The line and bus data are taken from the IEEE-30 bus system. A 32-MW wind power facility generates wind energy based on randomly generated wind speed. Ten turbines, each having a nominal capacity of 3.2 MW, with model SWT-3.2–113, are considered for the wind energy system. Then, Newton–Raphson load flow analysis is performed with and without considering the implementation of wind energy for 24 h, MOPSO and MOALO optimization techniques are used to minimize the multi-objective functions, and the results of the ideal solution are suitably saved. Load profile is shown in Table 1 and Figure 2, while optimal curves for IEEE 30-bus system are shown in Figures 3, 4.

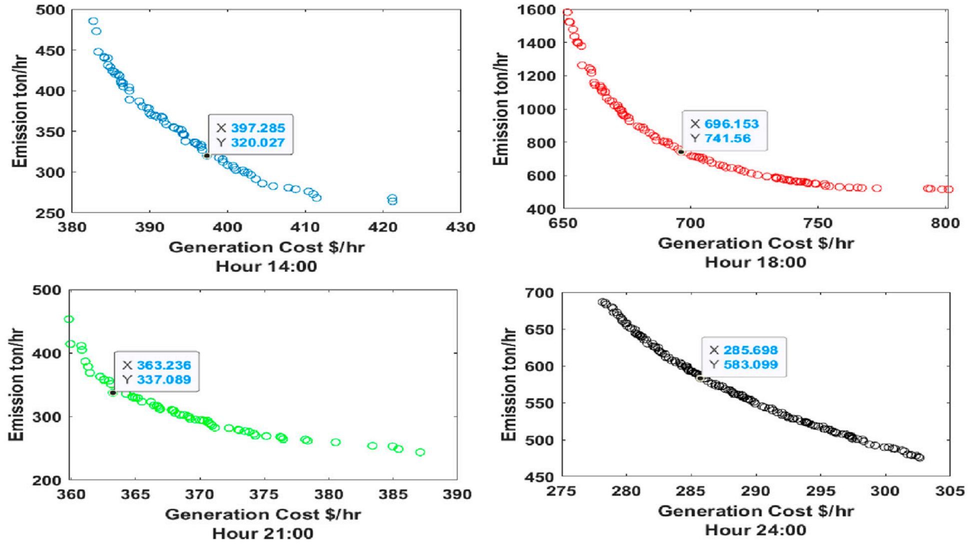

FIGURE 4
Pareto optimal curves for hours 14:00, 18:00, 21:00, and 24:00 in the IEEE-30 bus system (MOPSO).

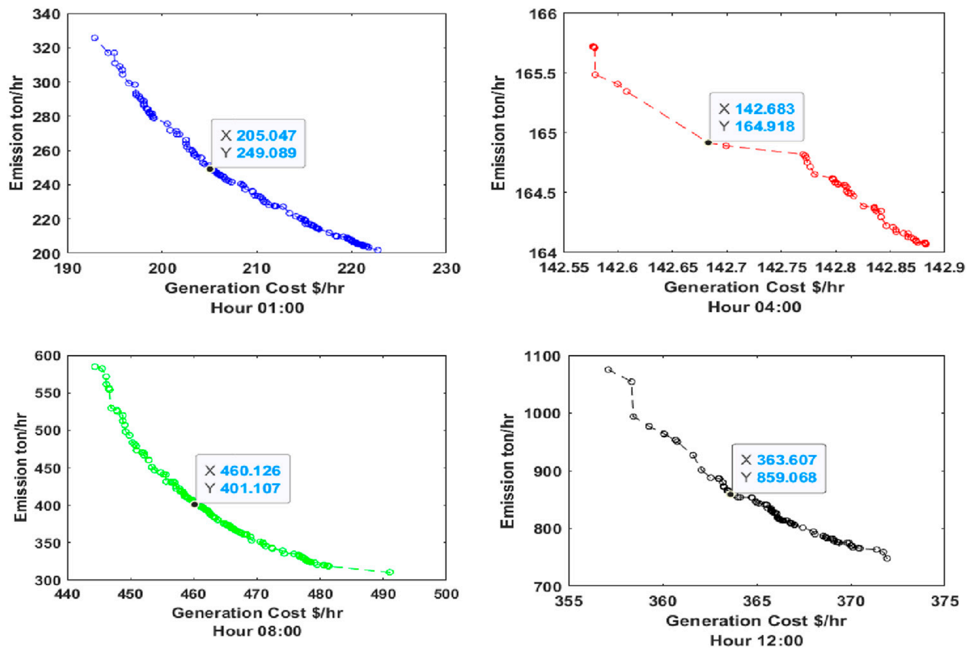

FIGURE 5
Pareto optimal curves for hours 01:00, 04:00, 08:00, and 12:00 in the IEEE-30 bus system (MOALO).

4 Results and discussion

4.1 Results and discussion

In this work, the standard IEEE-30 bus system is optimized using different multi-objective optimization techniques, daily load profile has been introduced by scaling of the load, wind power is generated using randomly generated wind speeds and wind turbine models, and different approaches are proposed and compared to observe the best results. Fuel cost and pollution are two objective functions that are minimized using the fuzzy min–max approach.

Parameters of multi-objective optimization techniques:

- Population size (Np) is set to 200.
- Random populations are generated by bus generator limits and bus voltage limits.
- Repository size (Nr) is set to 200.
- Maximum number of iterations is set to 200.

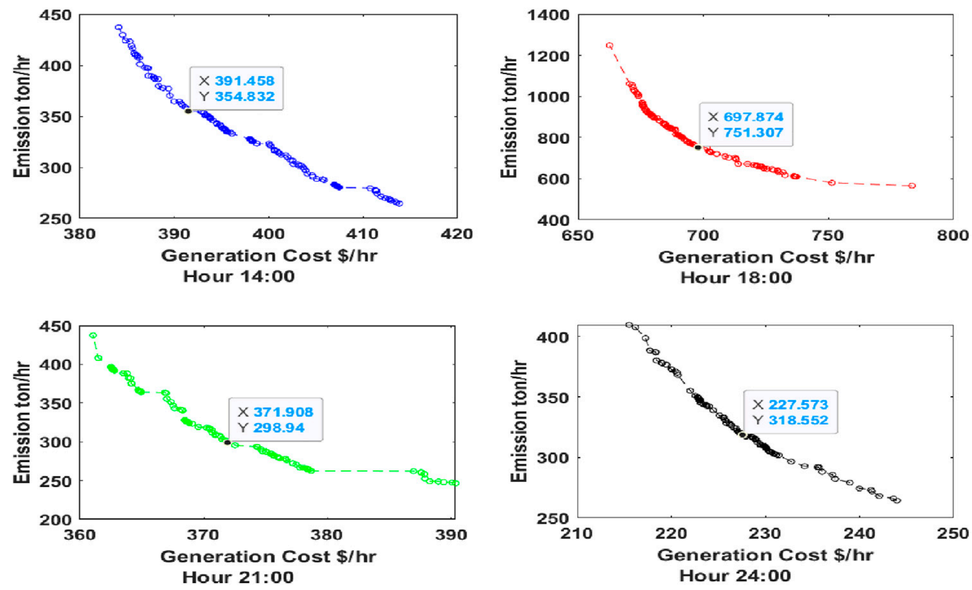

FIGURE 6
Pareto optimal curves for hours 14:00, 18:00, 21:00, and 24:00 in the IEEE-30 bus system (MOALO).

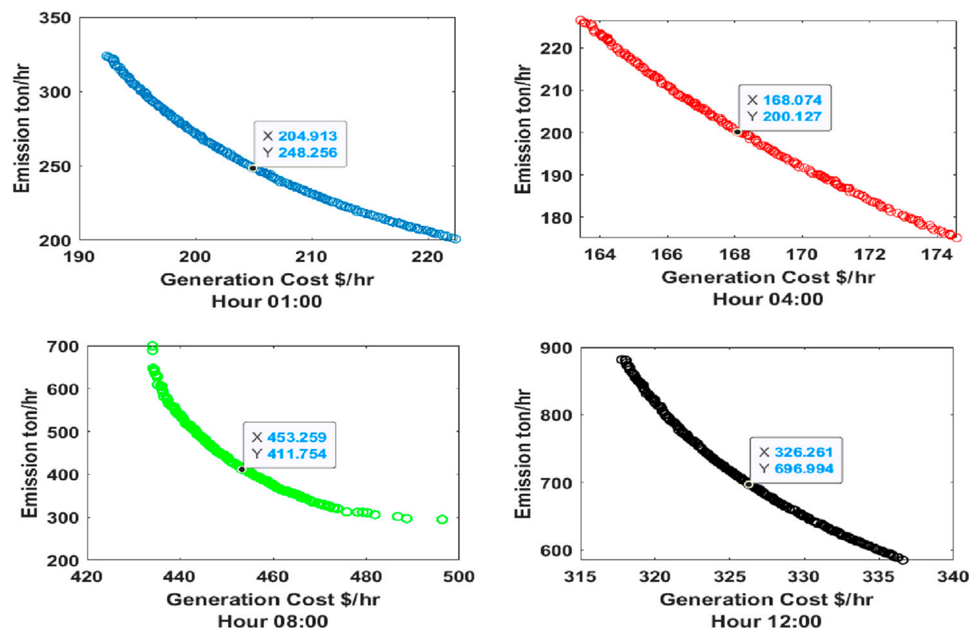

FIGURE 7
Pareto optimal curves with wind power implementation for hours 01:00, 04:00, 08:00, and 12:00 (MOPSO).

4.1.1 Case 1: implementation of the daily load profile for the IEEE-30 bus system

Daily load profiles have been implemented to the IEEE-30 bus system, multi-objective factors like generation costs and emissions are optimized using the multi-objective particle swarm optimization (MOPSO) and multi-objective ant lion optimization (MOALO) algorithms, and the fuzzy min–max approach has been used to get the best minimal results.

As demonstrated in the figure and table below, a daily load profile has been developed by scaling the IEEE-30 bus system load according to a real-time load profile for 24 h.

Due to the scaling of load, a condition is created to turn OFF some of the generators as the minimum limits of all the generators is 117 MW, and as the load/power demand ($P_{D,t}$) at some specific hours has decreased drastically, if all the generators are turned ON, the minimum limit of generators

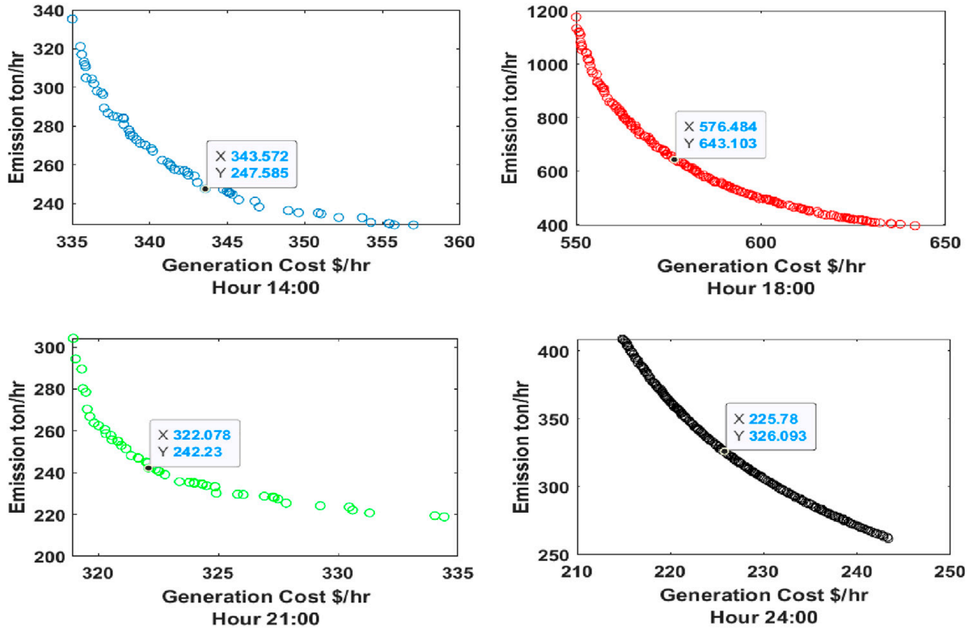

FIGURE 8
Pareto optimal curves with wind power implementation for hours 14:00, 18:00, 21:00, and 24:00 (MOPSO).

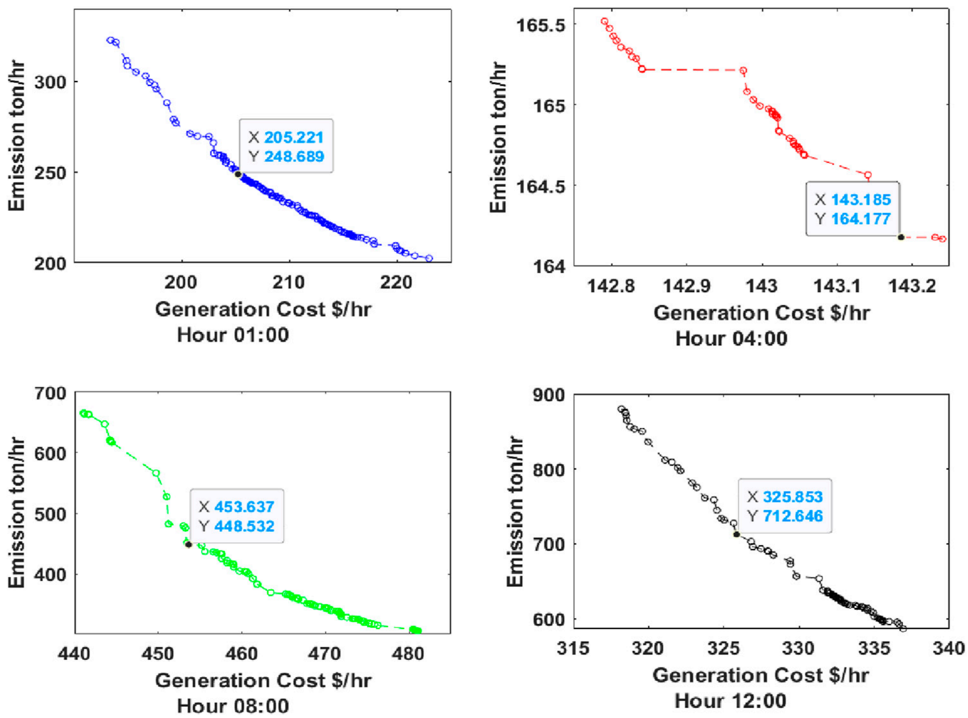

FIGURE 9
Pareto optimal curve with wind power implementation for hours 01:00, 04:00, 08:00, and 12:00 (MOALO).

would not be met, and a penalty factor would kick in, affecting the objectives. A condition as in Equation 12 must be imposed in which

$$G_t(\mathrm{ON}) = \begin{cases} G1, G5 & P_{D,t} < 117 \\ G1, G4 & 117 \le P_{D,t} < 140 \\ G1, G2, G3, G4, G5, G6 & P_{D,t} \ge 140 \end{cases}, \tag{12}$$

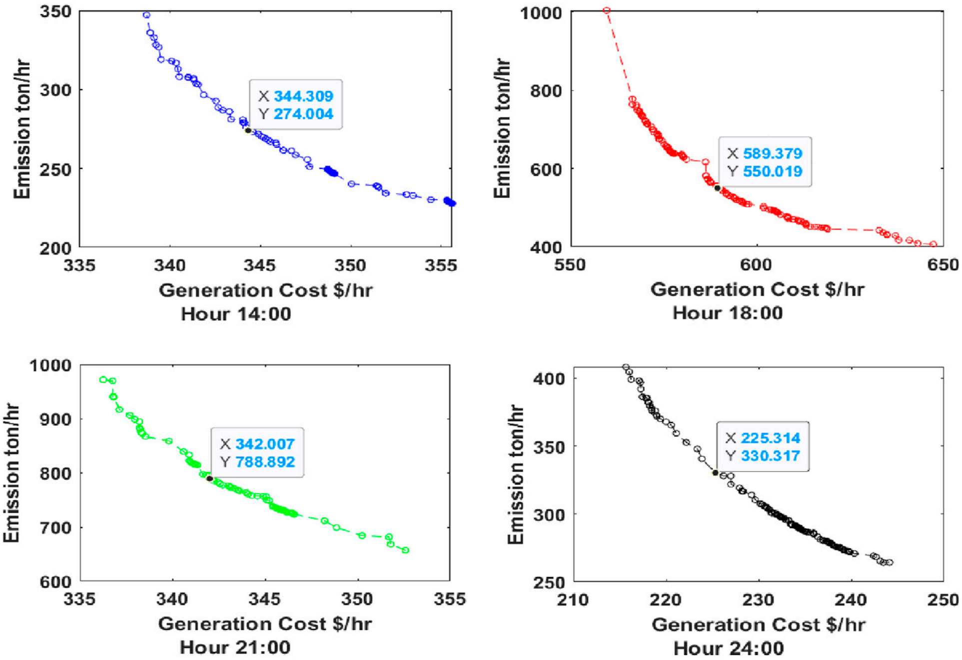

FIGURE 10
Pareto optimal curve with wind power implementation for hours 14:00, 18:00, 21:00, and 24:00 (MOALO).

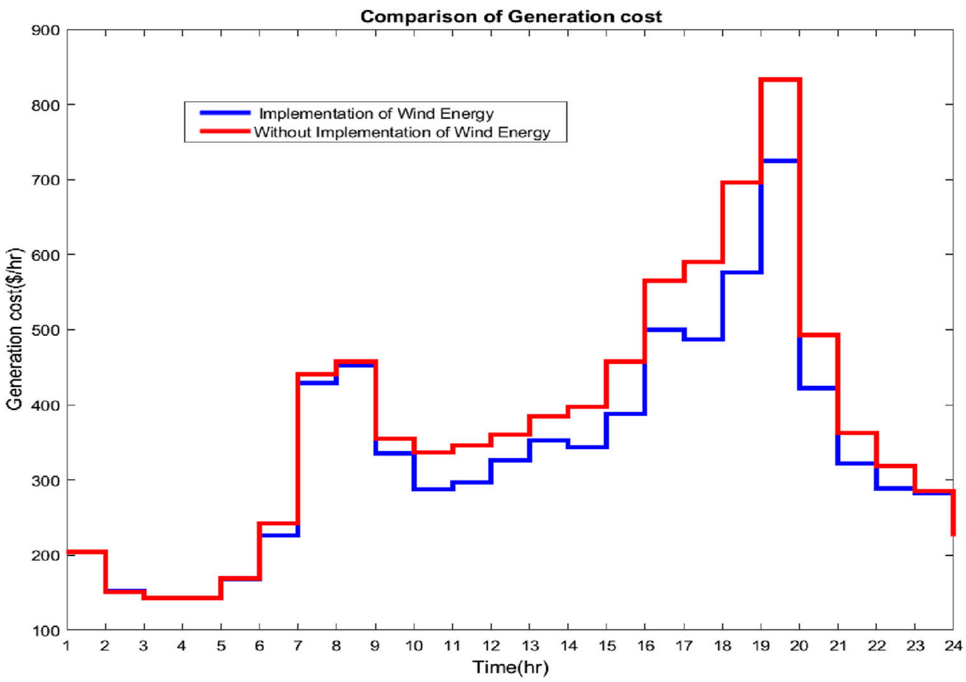

FIGURE 11
Comparison of generation costs with and without implementing wind energy using MOPSO.

where G_t (ON), G, and $P_{D,t}$ are generators turned ON, thermal power generator, and power demand, respectively, at time *t*.

From Table.2, 3 below, it has been observed that some of the generators are turned "OFF" to satisfy the constraints. The generation costs and emissions are optimized using MOPSO and MOALO, and the minimum point of the objectives is observed using the fuzzy min–max approach; the Pareto curves for 24 h for both the optimization techniques are given in Figures 5–12.

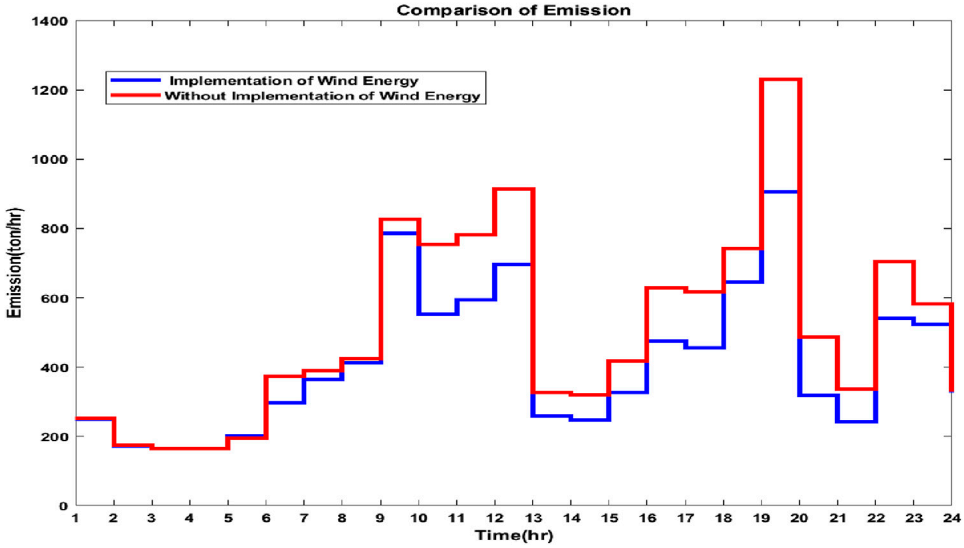

FIGURE 12
Comparison of emissions with and without implementing wind energy using MOPSO.

TABLE 6 Wind power generation for 24 h.

Time of the day (Hr)	Wind power generated (MW)	Time of the day (Hr)	Wind power generated (MW)
01:00	6.7396	13:00	11.955
02:00	3.3162	14:00	17.943
03:00	3.3162	15:00	22.349
04:00	6.3911	16:00	21.570
05:00	2.1588	17:00	32
06:00	6.3911	18:00	32
07:00	3.5423	19:00	32
08:00	1.1925	20:00	25.655
09:00	5.4180	21:00	15.5353
10:00	17.270	22:00	11.1443
11:00	16.614	23:00	1.9969
12:00	12.483	24:00	4.0247

4.1.2 Case 2: implementation of the daily load profile and wind energy in the IEEE-30 bus system

Wind energy has been implemented along with daily load profiles in the IEEE-30 bus system, multi-objective factors like generation cost and emission are optimized using the multi-objective particle swarm optimization (MOPSO) and multi-objective ant lion optimization (MOALO) algorithms, and the fuzzy min–max approach has been used to get the best minimal results.

Wind speed is randomly generated, and a 32-MW wind power source is generated using Equation 11 for this work. The wind energy is considered to be equipped using 10 turbine model SWT-3.2–113, with a nominal capacity of 3.2 MW. The specifications of wind turbines are given in Table 4. Wind speeds are tabulated in Table 5 while the wind power generated is shown in Table 6.

Given that wind speed is not constant, the rated power of 32 MW can be reached at any time of the day. However, if wind power generation is high, the minimum limits of the generators would not be met, and a penalty factor will take effect, which will have an impact on the objectives. Therefore, a condition as in Equation 13 has been imposed where

$$G_t\,(\mathrm{ON}) = \begin{cases} G1, G2 & P_{D,t} < 92 \\ G1, G2, P_{wind,t} & P_{D,t} \geq 92 \\ G1, G2, G3, G4, G5, G6, P_{wind,t} & P_{D,t} \geq 149 \end{cases}, \quad (13)$$

where G_t (ON), G, $P_{D,t}$,and $P_{wind,t}$ are generators turned ON, thermal power generator, power demand, and wind power generation, respectively, at time t.

When Equation 13 is satisfied, the wind energy sources are integrated, and the generation costs and emissions are significantly reduced, as shown in Tables 7, 8. The generation costs and emissions are optimized using MOPSO and MOALO, and the minimum point of the objectives is observed using the fuzzy min–max approach. The Pareto curves for 24 h for both the optimization techniques are given in Figures 7–10. Wind energy sources are not implemented for hours 1, 2, 3, 5, and 24 because Equation 13 is satisfied.

4.1.3 Case 3: comparison of results

From the results obtained from cases 1 and 2, it has been observed that for the optimization of both MOALO and MOPSO, the generation costs and emissions have been drastically reduced when wind energy is implemented into the system, that is, when Equation 13 is satisfied and is observed in Figures 11–16.

TABLE 7 Optimization of the IEEE-30 bus system with the implementation of wind energy using MOPSO.

Time (Hr)	G1 (MW)	G2 (MW)	G3 (MW)	G4 (MW)	G5 (MW)	G6 (MW)	Wind power (MW)	Power demand (MW)	Loss (MW)	Power generation (MW)	Generation cost ($/hr)	Emission (ton/hr)
01:00	59.9581	0	0	0	20.378	0	6.7396*	79.352	1.0691	80.3361	204.913	248.256
02:00	50.859	0	0	0	12.2344	0	3.3162*	62.348	0.826	63.0933	151.863	171.555
03:00	50.026	0	0	0	10.2179	0	3.3162*	59.514	0.7328	60.2438	142.7	164.174
04:00	50.1781	0	0	0	10.0626	0	2.1588*	59.514	0.7267	60.2407	168.074	200.127
05:00	54.7403	0	0	0	14.1232	0	6.3911*	68.016	0.8567	68.8635	142.517	165.018
06:00	65.2779	0	0	0	23.0401	0	6.3911	93.522	1.1901	94.7091	225.843	296.364
07:00	59.9598	39.6129	19.2437	20.1619	13.9687	12.4279	3.5423	167.2	1.7173	168.9173	429.42	364.976
08:00	65.2229	39.7248	20.8805	19.2189	14.6821	13.9238	1.1925	172.874	1.9745	174.8455	453.259	411.754
09:00	108.963	0	0	21.5007	0	0	5.418	133.198	2.6872	135.8822	336.183	784.88
10:00	90.8409	0	0	21.8345	0	0	17.27	127.53	2.4184	129.9454	287.565	551.532
11:00	94.4064	0	0	21.8494	0	0	16.614	130.364	2.5163	132.8698	297.227	594.228
12:00	102.149	0	0	24.0085	0	0	12.483	136.032	2.6112	138.6402	326.261	696.994
13:00	51.0486	32.2119	18.2165	14.0427	12.1217	12	11.955	150.202	1.3944	151.5964	352.277	258.081
14:00	50.1709	31.4551	17.3993	14.0216	11.0158	12.6137	17.943	153.036	1.5834	154.6194	343.572	247.585
15:00	57.5932	36.7736	20.8331	12.8715	12.6018	12	22.349	172.874	2.1584	175.0223	388.193	325.582
16:00	69.7464	42.1759	20.9582	24.8986	12.1298	18.1207	21.57	206.882	2.7278	209.5997	499.813	475.05
17:00	68.259	40.5798	21.2812	23.7416	16.1876	13.9861	32	212.55	3.4852	216.0352	487.275	453.387
18:00	83.2702	46.1782	21.9215	27.2275	19.7905	14.8384	32	240.89	4.358	245.2265	576.484	643.103
19:00	100.251	48.7821	24.8006	33.8508	23.8941	25.125	32	283.4	5.3038	288.7038	725.131	904.72
20:00	52.911	39.1469	20.9278	22.08	11	14.934	25.655	184.21	2.4556	186.6556	422.179	317.683
21:00	50.523	31.168	16.8134	10	10	12	15.5353	144.534	1.5154	146.0398	322.078	242.23
22:00	89.5829	0	0	23.2067	0	0	11.1443	121.862	2.0862	123.9339	289.173	539.635
23:00	88.1891	0	0	0	22.2044	0	1.9969	110.526	1.8674	112.3904	281.819	521.595
24:00	69.5145	0	0	0	19.6028	0	4.0247*	87.854	1.2663	89.1173	225.78	326.093

TABLE 8 Optimization of the IEEE-30 bus system with the implementation of wind energy using MOALO.

Time (Hr)	G1 (MW)	G2 (MW)	G3 (MW)	G4 (MW)	G5 (MW)	G6 (MW)	Wind power (MW)	Power demand (MW)	Loss (MW)	Power generation (MW)	Generation cost ($/hr)	Emission (ton/hr)
01:00	60.0025	0	0	0	20.4276	0	6.7396*	79.352	1.0842	80.4301	205.221	248.689
02:00	51.3834	0	0	0	11.7104	0	3.3162*	62.348	0.8305	63.0938	151.227	174.457
03:00	50.0497	0	0	0	10.1247	0	3.3162*	59.514	0.7577	60.1744	142.43	164.244
04:00	50.0055	0	0	0	10.3696	0	2.1588*	59.514	0.864	60.375	143.185	164.177
05:00	53.8599	0	0	0	15.0501	0	6.3911*	68.016	0.894	68.91	169.411	195.163
06:00	66.0857	0	0	0	22.3055	0	6.3911	93.522	1.2633	94.7824	225.191	301.716
07:00	61.2473	37.9578	20.5807	15.6789	15.7659	14.1687	3.5423	167.206	1.7502	168.9417	429.299	367.287
08:00	73.7386	28.7489	21.0763	17.5366	12.9601	19.8793	1.1925	172.874	2.28	175.1324	453.637	448.532
09:00	107.668	0	0	22.8148	0	0	5.418	133.198	2.706	135.901	337.297	769.345
10:00	87.1598	0	0	25.5051	0	0	17.27	127.53	2.4079	129.9349	291.125	516.992
11:00	93.4057	0	0	22.8582	0	0	16.614	130.964	2.5235	132.8779	298.176	584.104
12:00	103.536	0	0	22.828	0	0	12.483	136.032	2.8209	138.847	325.853	712.646
13:00	61.5642	29.8908	15.0169	11.5375	10	12.1907	11.955	150.202	1.9589	152.155	345.791	316.358
14:00	57.808	22.0229	16.8302	11.6415	13.6926	14.7985	17.943	153.036	1.7105	154.7367	344.309	274.004
15:00	61.9617	32.1941	17.3853	15.4345	11.4777	14.7775	22.349	172.874	2.7159	175.5798	388.742	339.536
16:00	61.7093	41.1245	22.1059	27.7646	15.7998	19.2166	21.57	206.882	2.4087	209.2907	509.097	417.169
17:00	61.3886	41.6095	23.6185	19.4603	18.2623	19.4822	32	212.55	3.2814	215.8214	495.972	406.834
18:00	72.2004	45.4997	25.4244	30.4568	18.6492	20.595	32	240.89	3.941	244.8255	589.379	550.019
19:00	92.8755	53.0902	29.9234	31.993	23.3505	25.1731	32	283.4	5.1265	288.4058	733.775	844.738
20:00	62.8957	31.1608	21.3619	20.6811	12.68	12.4159	25.655	184.21	2.7244	186.8503	415.974	358.746
21:00	109.028	0	0	23.0585	0	0	15.25353	144.534	3.1142	147.6217	342.007	788.892
22:00	90.681	0	0	22.1773	0	0	11.1443	121.862	2.1406	124.0026	288.377	550.331
23:00	90.056	0	0	20.4536	0	0	1.9969	110.526	1.3348	112.5065	280.488	539.752
24:00	69.9934	0	0	0	19.2352	0	4.0247*	87.854	1.3746	89.2286	225.314	330.317

10.3389/fenrg.2024.1421212

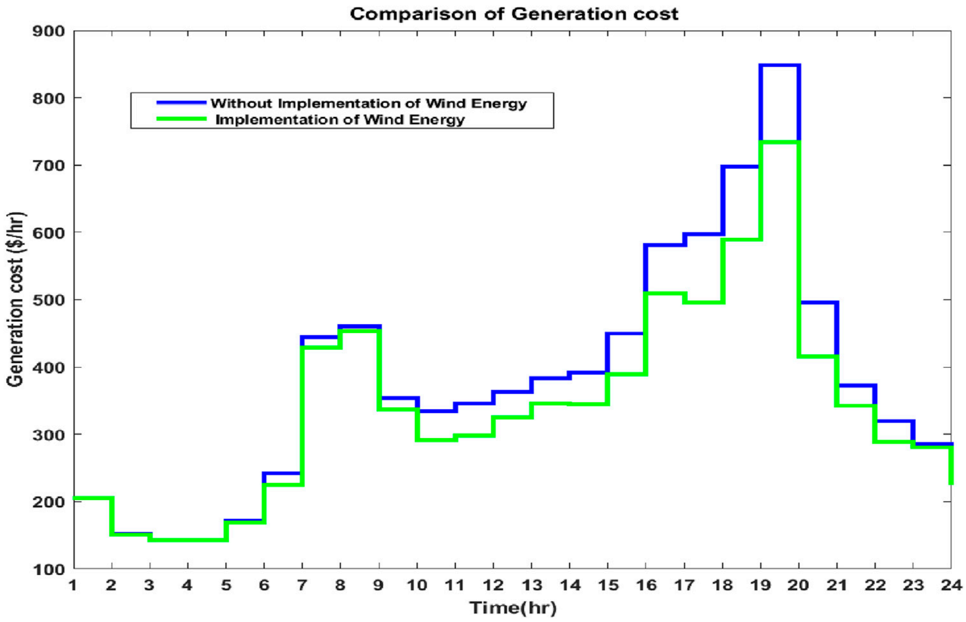

FIGURE 13
Comparison of generation costs with and without implementing wind energy using MOALO.

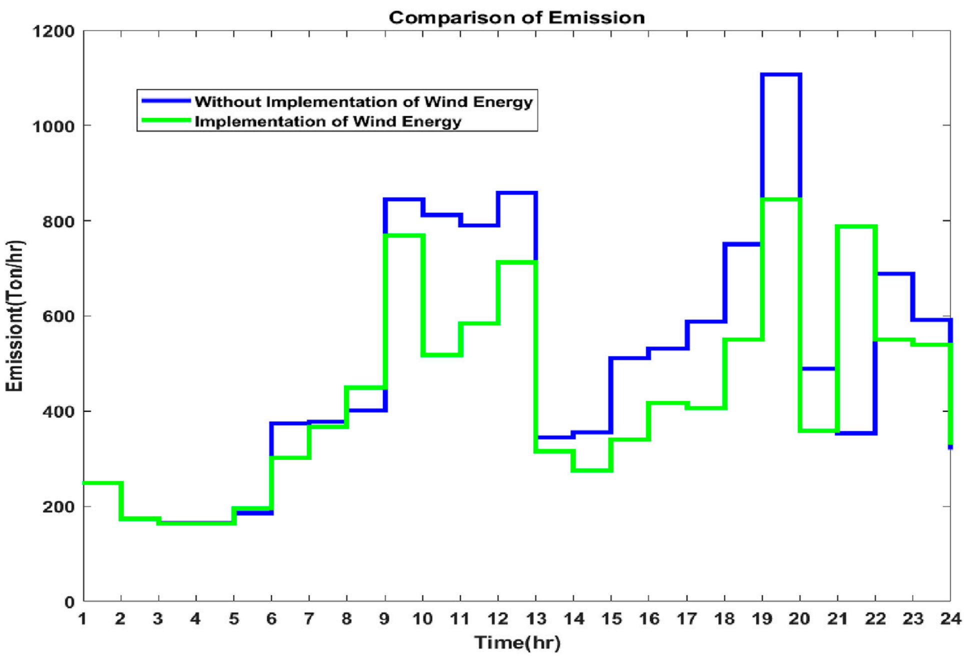

FIGURE 14
Comparison of emissions with and without implementing wind energy using MOALO.

For comparison of the optimization algorithms, the total generation costs, and emissions for 24 h, it has been observed that for Case 1, MOPSO has lower total generation costs with a difference of $42.763. However, MOALO has the lower emission with a difference of 157.337 tons and is shown in Figures 15A, B. For Case 2, with the implementation of wind energy, MOPSO has lower total generation costs with a difference of $51.678 and lower emissions with a difference of 459.446 tons and is observed in Figures 16A, B.

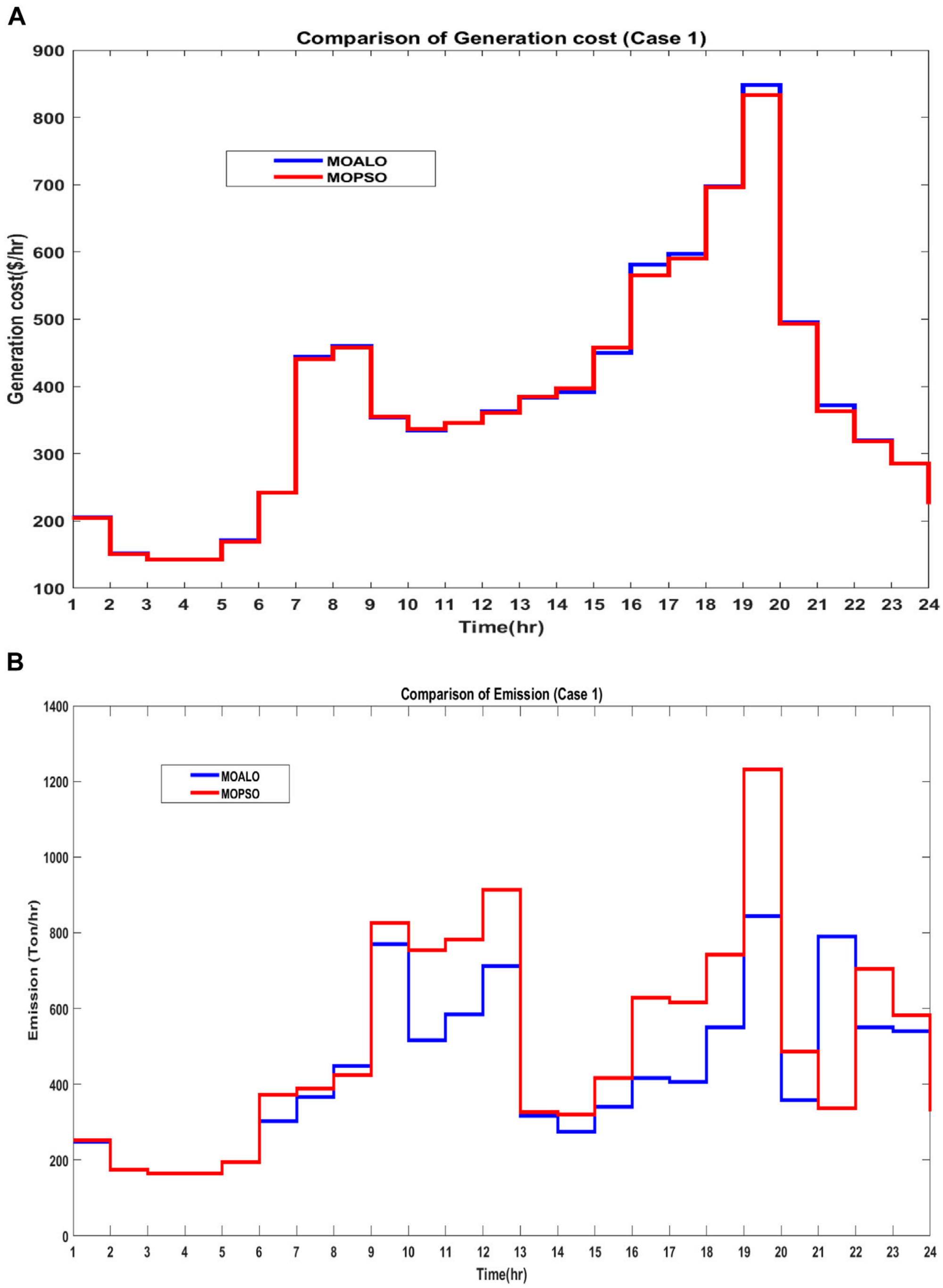

FIGURE 15
(A) Comparison of generation costs using MOPSO and MOALO for case 1 and **(B)** comparison of emissions using MOPSO and MOALO for case 1.

5 Conclusion

In this work, a daily load profile was applied to the IEEE-30 bus system to analyze economic dispatch (ED) problems, both with and without wind energy sources. Multi-objective optimization methods were utilized to balance generation costs and emissions. Wind energy was generated for 24 h using random wind speeds, and it was observed that the incorporation of wind energy led to significant reductions in both generation costs and emissions over the entire period.

To optimize economic generation cost and emission dispatch, multi-objective ant lion optimization (MOALO) and multi-objective particle swarm optimization (MOPSO) were employed. The fuzzy min–max technique was used to identify the optimal minimum outcomes. It was found that MOPSO

10.3389/fenrg.2024.1421212

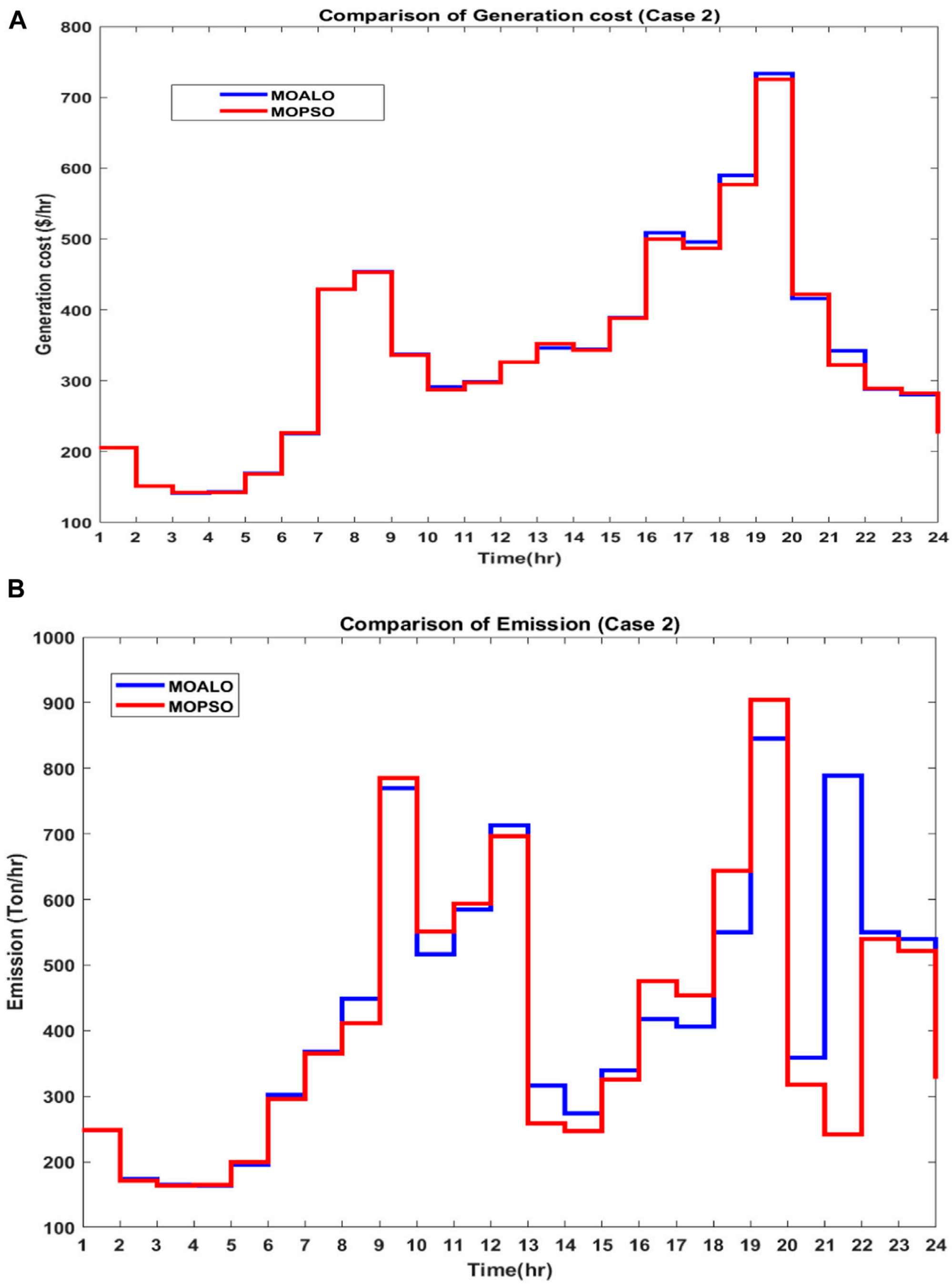

FIGURE 16
(A) Comparison of generation costs using MOPSO and MOALO for case 2 and **(B)** comparison of emissions using MOPSO and MOALO for case 2.

outperformed MOALO in effectively minimizing both objectives.

For future research, the integration of additional renewable energy sources, such as solar and hydroelectric power, is recommended to further enhance the results of the proposed optimization. The inclusion of electric vehicles in the vehicle-to-grid (V2G) mode as a renewable power source should also be considered. Furthermore, the investigation of other advanced optimization algorithms and novel control strategies could provide additional improvements in managing generation costs and emissions. Additionally, exploring deregulated energy markets may offer valuable insights into optimizing economic dispatch and emissions within different market structures.

Data availability statement

The original contributions presented in the study are included in the article/Supplementary Material, further inquiries can be directed to the corresponding authors.

Author contributions

RL: writing–original draft, writing–review and editing, conceptualization, investigation. SHD: writing–original draft, writing–review and editing, conceptualization, investigation. SID: writing–original draft, writing–review and editing, conceptualization, investigation. KS: writing–original draft, writing–review and editing, conceptualization, investigation. UC: writing–original draft, writing–review and editing, conceptualization, investigation. TU: writing–original draft, writing–review and editing, conceptualization, investigation.

Funding

The author(s) declare that no financial support was received for the research, authorship, and/or publication of this article.

Conflict of interest

The authors declare that the research was conducted in the absence of any commercial or financial relationships that could be construed as a potential conflict of interest.

Publisher's note

Supplementary material

The Supplementary Material for this article can be found online at: https://www.frontiersin.org/articles/10.3389/fenrg.2024.1421212/full#supplementary-material

References

Abdolrasol, M., G. M., Hannan, M. A., Hussain, S. M. S., Sarker, M. R., and Ker, P. J. (2021). Energy management scheduling for microgrids in the virtual power plant system using artificial neural networks. *Energies* 14, 6507. wind solar. doi:10.3390/en14206507

Badran, O., and Abdulhadi, E. (2009). Evaluation of factors affecting wind power generation in Jordan. *Seventh Asia-Pacific Conf. Wind Eng.*

Barik, A. K., Das, D. C., Latif, A., Hussain, S. M. S., and Ustun, T. S. (2021). Optimal voltage–frequency regulation in distributed sustainable energy-based hybrid microgrids with integrated resource planning. *Energies* 14, 2735. doi:10.3390/en14102735

Basu, J. B., Dawn, S., Saha, P. K., Chakraborty, M. R., and Ustun, T. S. (2022). Economic enhancement of wind–thermal–hydro system considering imbalance cost in deregulated power market. *Sustainability* 14, 15604. challenges. doi:10.3390/su142315604

Bencherif, M., Brahmi, B. N., and Chikhhaoui, A. (2014). Optimum selection of wind turbines. *Sci. J. Energy Eng.* 2 (4), 36–46.

Bianchi, F. D., Battista, H. D., and Mantz, R. J. (2007). *Wind turbine control systems*. Germany: Springer, 7.

Burton, T., Jenkins, N., Sharpe, D., and Bossanyi, E. (2011). *"Wind energy handbook", book*. John Wiley & Sons, Ltd.

Chatuanramtharnghaka, B., and Deb, S. (2020). "Multi-objective particle Swarm optimization based congestion management considering generation rescheduling and cost minimization," in *International conference on advances in computing, communication & materials (ICACCM)-2020*. Dehradun, India: Tula's Institute, 21–22 August 2020.

Chauhan, A., Upadhyay, S., Khan, M. T., Hussain, S. M. S., and Ustun, T. S. (2021). Performance investigation of a solar photovoltaic/diesel generator based hybrid system with cycle charging strategy using BBO algorithm. *Sustainability* 13, 8048. doi:10.3390/su13148048

Chen, G., Qian, J., Zhang, Z., and Sun, A. Z. (2019). Multi-objective optimal power flow based on hybrid firefly-bat algorithm and constraints prior object-fuzzy sorting strategy. *IEEE Trans. Evol. Comput.* 7, 139726–139745. doi:10.1109/access.2019.2943480

Coello Coello, A., Toscano Pulido, G., and Salazar Lechuga, M. (2004). Handling multiple objectives with particle Swarm optimization. *IEEE Trans. Evol. Comput.* 8 (3), 256–279. doi:10.1109/tevc.2004.826067

Das, A., Dawn, S., Gope, S., and Ustun, T. S. (2022). A risk curtailment strategy for solar PV-battery integrated competitive power system. *Electronics* 11, 1251. doi:10.3390/electronics11081251

Dey, P. P., Das, D. C., Latif, A., Hussain, S. M. S., and Ustun, T. S. (2020). Active power management of virtual power plant under penetration of central receiver solar thermal-wind using butterfly optimization technique. *Sustainability* 12, 6979. doi:10.3390/su12176979

El-Ahmar, M. H., Abou-Hashema, M., El-Sayed, and Hemeida, A. M. (2017). *Evaluation of factors affecting wind turbine output power*. Egypt: Menoufia University.

Farooq, Z., Rahman, A., Hussain, S. M. S., and Ustun, T. S. (2022). Power generation control of renewable energy based hybrid deregulated power system. *Energies* 15, 517. doi:10.3390/en15020517

Ghasemi, M., Ghavidel, S., Akbari, E., and Vahed, A. A. (2014). Solving nonlinear, non-smooth and non-convex optimal power flow problems using chaotic invasive weed optimization algorithms based on chaos. " *Energy* 73, 340–353. doi:10.1016/j.energy.2014.06.026

Hamoudi, Y., Amimeur, H., Aouzellag, D., Abdolrasol, M. G. M., and Ustun, T. S. (2023). Hyperparameter bayesian optimization of Gaussian process regression applied in speed-sensorless predictive torque control of an autonomous wind energy conversion system. *Energies* 16, 4738. doi:10.3390/en16124738

Hoang Bao Huy, T., Kim, D., and Ngoc, D. (2022). Multi-objective optimal power flow using multiobjective search group algorithm. *IEEE Trans. Evol. Comput.* 10, 77837–77856. doi:10.1109/access.2022.3193371

Hussain, I., Das, D. C., Sinha, N., Latif, A., Hussain, S. M. S., and Ustun, T. S. (2020). Performance assessment of an islanded hybrid power system with different storage combinations using an FPA-tuned two-degree-of-freedom (2DOF) controller. *Energies* 13, 5610. doi:10.3390/en13215610

Johnson, G. L. (1985). *Wind energy systems*. Englewood Cliffs, NJ, USA: Prentice-Hall, 147–149.

Kala, H., and Sandhu, K. S. (2016). "Performance analysis of wind turbines with different ratings for site matching," in *1st IEEE intern. Conf. On power electronics, intell. Cont. And energy systems (ICPEICES)*.

Kanchikere, J. (2012). Aerodynamic factors affecting wind turbine power generation. *Intern. J. Eng. Res. & Techn. (IJERT)* 1 (issue-9).

Khalfallah, M. G., and Koliub, A. M. (2007). Suggestions for improving wind turbines power curves. *Desalination* 209, 221–229. doi:10.1016/j.desal.2007.04.031

Khan, H. (2009). *Non-Conventional energy sources*. 2nd ed. New Delhi: Tata McGraw-Hill.

Kulworawanichpong, T. (2010). ""Simplified Newton–Raphson power-flow solution method" power system research unit," in *School of electrical engineering*. Thailand: Institute of Engineering, 111 University Avenue, Suranaree University of Technology. Nakhon Ratchasima 30000.

Latif, A., Hussain, S. M. S., Das, D. C., and Ustun, T. S. (2021). Optimization of two-stage IPD-(1+I) controllers for frequency regulation of sustainable energy based hybrid microgrid network. *Electronics* 10, 919. doi:10.3390/electronics10080919

Latif, A., Paul, M., Das, D. C., Hussain, S. M. S., and Ustun, T. S. (2020). Price based demand response for optimal frequency stabilization in ORC solar thermal based isolated hybrid microgrid under Salp Swarm technique. *Electronics* 9, 2209. doi:10.3390/electronics9122209

Manwell, J. F., McGowan, J. G., and Rogers, A. L. (2010). *Wind energy explained: theory, design and application*. Hoboken, NJ, USA: Wiley.

Marimuthu, C., and Kirubakaran, V. (2014). A critical review of factors affecting wind turbine and solar cell system power production. *Intern. Jour. Adv. Eng. Res. Stu.*, 143–147.

Mirjalili, S., Jangir, P., and Saremi, S. (2016). Multi-objective ant lion optimizer: a multi-objective optimization algorithm for solving engineering problems. *Appl. Intell.* 46, 79–95. doi:10.1007/s10489-016-0825-8

Nayak, S. R., Khadanga, R. K., Panda, S., Sahu, P. R., Padhy, S., and Ustun, T. S. (2023). Participation of renewable energy sources in the frequency regulation issues of a five-area hybrid power system utilizing a sine cosine-adopted african vulture optimization algorithm. *Energies* 16 (16), 926. doi:10.3390/en16020926

Nemes, C., and Munteanu, F. (2012). Operational parameters evaluation for optimal wind energy systems development. *U.P.B. Sci. Bull. Ser. C* 74 (Issue-1), 223–230.

Niu, M., Wan, C., and Xu, Z. (2014). A review on applications of heuristic optimization algorithms for optimal power flow in modern power systems. ” *J. Mod. Power Syst. Clean. Energy* 2 (4), 289–297. doi:10.1007/s40565-014-0089-4

Safiullah, S., Rahman, A., Lone, S. A., Hussain, S. M. S., and Ustun, T. S. (2022). Novel COVID-19 based optimization algorithm (C-19BOA) for performance improvement of power systems. *Sustainability* 14, 14287. doi:10.3390/su142114287

Salih, S. M., Taha, M. Q., and Alawsaj, M. K. (2012). Performance analysis of wind turbine systems under different parameters effect. *Int. J. Energy Environ. (IJEE)* 3 (Issue-6), 895–904.

Singh, N. K., Koley, C., Gope, S., Dawn, S., and Ustun, T. S. (2021). An economic risk analysis in wind and pumped hydro energy storage integrated power system using meta-heuristic algorithm. *Sustainability* 13, 13542. doi:10.3390/su132413542

Srinivasan, R., Sridhar, M., Suresh, A., Mominul, H., Julfikar, I., and Minarul, Md. (2023). Hybrid social grouping algorithm-perturb and observe power tracking scheme for partially shaded photovoltaic array. *Int. J. Energy Res.*, 18.

Surender Reddy, S. (2018). Multi-objective optimization considering cost, emission and loss objectives using PSO and fuzzy approach. *Int. J. Eng. & Technol.* 7, 1552. doi:10.14419/ijet.v7i3.11203

Ulutas, A., Altas, I. H., Onen, A., and Ustun, T. S. (2020). Neuro-fuzzy-based model predictive energy management for grid connected microgrids. *Electronics* 9, 900. doi:10.3390/electronics9060900

Ustun, T. S., Ozansoy, C., and Zayegh, A. (2011). “Distributed energy resources (DER) object modeling with IEC 61850–7–420,” in *Aupec 2011*. Brisbane, QLD, Australia, 1–6.

Wiratama, I. K., Mara, I. M., and Nuarsa, I. M. (2016). Investigation of factors affecting power curve wind turbine blade. *ARPN J. Eng. Appl. Sci.* 11 (4), 2759–2762.

Yarar, N., Yagci, M., Bahceci, S., Onen, A., and Ustun, T. S. (2023). Artificial neural networks based harmonics estimation for real university microgrids using hourly solar irradiation and temperature data. *Energy Nexus* 9, 100172. doi:10.1016/j.nexus.2023.100172

Zhang, J., Tang, Q., Li, P., Deng, D., and Chen, Y. (2016). A modified MOEA/D approach to the solution of multi-objective optimal power flow problem. ” *Appl. Soft Comput.* 47, 494–514. doi:10.1016/j.asoc.2016.06.022